

# Evaluation of trabecular meshwork-specific promoters *in vitro* and *in vivo* using scAAV2 vectors expressing C3 transferase

Jun-Kai Tan<sup>1</sup>, Ying Xiao<sup>2</sup>, Guo Liu<sup>3</sup>, Long-Xiang Huang<sup>4</sup>, Wen-Hao Ma<sup>5</sup>, Yan Xia<sup>5</sup>, Xi-Zhen Wang<sup>6</sup>, Xian-Jun Zhu<sup>3</sup>, Su-Ping Cai<sup>6</sup>, Xiao-Bing Wu<sup>5</sup>, Yun Wang<sup>6</sup>, Xu-Yang Liu<sup>1,7</sup>

<sup>1</sup>Xiamen Eye Center, Xiamen University, Xiamen 361004, Fujian Province, China

<sup>2</sup>Department of Pathology, Hospital of Chengdu University of Traditional Chinese Medicine, Chengdu 610032, Sichuan Province, China

<sup>3</sup>Sichuan Provincial Key Laboratory for Human Disease Gene Study, Sichuan Provincial People's Hospital, University of Electronic Science and Technology of China, Chengdu 610072, Sichuan Province, China

<sup>4</sup>The First Affiliated Hospital of Fujian Medical University, Fuzhou 350004, Fujian Province, China

<sup>5</sup>Beijing FivePlus Molecular Medicine Institute Co., Ltd., Beijing 102600, China

<sup>6</sup>Shenzhen Key Laboratory of Ophthalmology, Shenzhen Eye Hospital, School of Optometry, Jinan University, Shenzhen 518040, Guangdong Province, China

<sup>7</sup>Department of Ophthalmology, Shenzhen People's Hospital, the 2<sup>nd</sup> Clinical Medical College, Jinan University, Shenzhen 518020, Guangdong Province, China

**Co-first authors:** Jun-Kai Tan, Ying Xiao, and Guo Liu

**Correspondence to:** Xu-Yang Liu. Xiamen Eye Center, Xiamen University, Xiamen 361004, Fujian Province, China. xliu1213@126.com; Yun Wang. Shenzhen Eye Hospital, Jinan University, Shenzhen Eye Institute, Shenzhen 518040, Guangdong Province, China. s\_ywang@126.com; Xiao-Bing Wu. Beijing FivePlus Molecular Medicine Institute Co., Ltd., Beijing 102600, China. wuxb0168@vip.sina.com

Received: 2022-12-15 Accepted: 2023-03-14

## Abstract

• **AIM:** To evaluate the potential of two trabecular meshwork (TM)-specific promoters, Chitinase 3-like 1 (Ch3L1) and matrix gla protein (MGP), for improving specificity and safety in glaucoma gene therapy based on self-complementary AAV2 (scAAV2) vector technologies.

• **METHODS:** An scAAV2 vector with C3 transferase (C3) as the reporter gene (scAAV2-C3) was selected. The scAAV2-C3 vectors were driven by Ch3L1 (scAAV2-Ch3L1-C3), MGP

(scAAV2-MGP-C3), enhanced MGP (scAAV2-eMGP-C3) and cytomegalovirus (scAAV2-CMV-C3), respectively. The cultured primary human TM cells were treated with each vector at different multiplicities of infections. Changes in cell morphology were observed by phase contrast microscopy. Actin stress fibers and Rho GTPases/Rho-associated protein kinase pathway-related molecules were assessed by immunofluorescence staining, real-time quantitative polymerase chain reaction and Western blot. Each vector was injected intracamerally into the one eye of each rat at low and high doses respectively. *In vivo* green fluorescence was visualized by a Micron III Retinal Imaging Microscope. Intraocular pressure (IOP) was monitored using a rebound tonometer. Ocular responses were evaluated by slit-lamp microscopy. Ocular histopathology analysis was examined by hematoxylin and eosin staining.

• **RESULTS:** In TM cell culture studies, the vector-mediated C3 expression induced morphologic changes, disruption of actin cytoskeleton and reduction of fibronectin expression in TM cells by inhibiting the Rho GTPases/Rho-associated protein kinase signaling pathway. At the same dose, these changes were significant in TM cells treated with scAAV2-CMV-C3 or scAAV2-Ch3L1-C3, but not in cells treated with scAAV2-eMGP-C3 or scAAV2-MGP-C3. At low-injected dose, the IOP was significantly decreased in the scAAV2-Ch3L1-C3-injected eyes but not in scAAV2-MGP-C3-injected and scAAV2-eMGP-C3-injected eyes. At high-injected dose, significant IOP reduction was observed in the scAAV2-eMGP-C3-injected eyes but not in scAAV2-MGP-C3-injected eyes. Similar to scAAV2-CMV-C3, scAAV2-Ch3L1-C3 vector showed efficient transduction both in the TM and corneal endothelium. In anterior segment tissues of scAAV2-eMGP-C3-injected eyes, no obvious morphological changes were found except for the TM. Inflammation was absent.

• **CONCLUSION:** In scAAV2-transduced TM cells, the promoter-driven efficiency of Ch3L1 is close to that of cytomegalovirus, but obviously higher than that of MGP. In the anterior chamber of rat eye, the transgene expression

pattern of scAAV2 vector is presumably affected by MGP promoter, but not by Ch3L1 promoter. These findings would provide a useful reference for improvement of specificity and safety in glaucoma gene therapy using scAAV2 vector.

● **KEYWORDS:** self-complementary AAV2; chitinase 3-like 1; matrix gla protein; trabecular meshwork; C3 transferase

**DOI:10.18240/ijo.2023.08.03**

**Citation:** Tan JK, Xiao Y, Liu G, Huang LX, Ma WH, Xia Y, Wang XZ, Zhu XJ, Cai SP, Wu XB, Wang Y, Liu XY. Evaluation of trabecular meshwork-specific promoters *in vitro* and *in vivo* using scAAV2 vectors expressing C3 transferase. *Int J Ophthalmol* 2023;16(8):1196-1209

## INTRODUCTION

Elevated intraocular pressure (IOP) is considered as a major risk factor in the progression of glaucomatous optic nerve deterioration. Currently, proper IOP-lowering treatments remain the major therapeutic strategy to prevent or slow down the progressive vision loss for glaucoma<sup>[1-2]</sup>. The trabecular meshwork (TM) is one of the main structural components of the conventional outflow pathway, playing an important role in formation and modulation of aqueous humor outflow resistance and IOP of the eye<sup>[3]</sup>. Therefore, there is an increasing interest and need in developing the IOP-lowering gene therapy approaches with long-term TM-targeted effects. Previous studies have tested several therapeutic genes delivered intracamerally by different viral vectors in order to lower IOP in living animals<sup>[4-12]</sup>. In these studies, gene transfer into the anterior segment has been performed using expression vectors driven by the cytomegalovirus (CMV) promoter, which delivers high and broad-spectrum transgene expression in a different tissues of anterior segment of the eye. As shown in our previous studies, intracameral delivery of the CMV-driven vectors expressing C3 transferase (C3), a protein capable of disrupting actin cytoskeleton by inhibiting Rho GTPase (Rho)/Rho-associated kinase (ROCK) pathway and facilitating aqueous humor outflow *via* TM, transduced not only TM, but also corneal endothelium and/or iris in the monkey eyes<sup>[4,9]</sup>. Consequently, some undesirable side effects were found in the tissues other than TM to varying degrees. To avoid undesirable viral vector transduction of ocular tissue, it is critically necessary to identify specific promoters by which the transgene specifically expresses in TM.

Chitinase 3-like 1 (Ch3L1) and matrix gla protein (MGP) were previously confirmed as the tissue specific markers of human TM cells<sup>[13-15]</sup>. In these studies, the expression of  $\beta$ -galactosidase was specifically restricted in the TM of human perfused anterior segment organ culture after delivery of recombinant adenoviruses containing the *LacZ* gene driven by

either MGP promoter or Ch3L1 promoter. This result indicates that the tissue-specific transgene expression can be controlled by use of different promoters.

In the present study, we evaluated the efficacy and specificity of Ch3L1 and MGP promoters, when compared to CMV, to promote C3 gene expression in the TM *in vivo* and *in vitro* using recombinant self-complementary AAV2 (scAAV2) vector. This study would provide a useful reference for improvement of specificity and safety in glaucoma gene therapy using scAAV2 vector.

## MATERIALS AND METHODS

**Ethical Approval** All animals were maintained and handled in accordance with the Association for Research in Vision and Ophthalmology (ARVO) statement for the Use of Animals in Ophthalmic and Vision Research. Study protocol was approved by Institutional Animal Care and Use Committee of Sichuan Provincial People's Hospital (AE-14/01.01).

**Viral Vectors** Recombinant scAAV2 vectors expressing either enhanced green fluorescent protein (eGFP) or C3 protein, was prepared by the Beijing Five-plus Molecular Medicine Institute (Beijing, China). Expressions from these scAAV2 vectors were driven by CMV (scAAV2-CMV-C3; scAAV2-CMV-eGFP), MGP (Figure 1; scAAV2-MGP-C3), enhanced MGP (scAAV2-eMGP-C3), Ch3L1 (scAAV2-Ch3L1-C3; Figure 1) and CAG (a combination of chicken beta-actin promoter and CMV immediate-early enhancer; scAAV2-CAG-eGFP) promoter, respectively. Briefly, the pscAAV-CAM (a human CMV enhancer with a chicken beta-actin promoter and mouse parvovirus intron) plasmid was constructed using pAAV2neo<sup>[16]</sup> as a precursor plasmid. The pscAAV-CAM was used as the basis for the construction of pscAAV-CAM-C3 plasmid. The human *Ch3L1* gene with restriction sites and pscAAV-CAM-C3 were digested with *XhoI/KpnI* (New England Biolabs, Ipswich, MA, USA) and ligated together. The human *MGP* gene with restriction sites and pscAAV-CAM-C3 were also digested with *XhoI/KpnI* and then ligated. The eMGP promoter was a modified version of the MGP promoter and designed by the Beijing Five-plus Molecular Medicine Institute. Next, the ligation products were transformed into *Escherichia coli* JM109 (Takara Bio, Dalian, China) for further replication. The subsequent processes including preparation, identification, purification, and titer determination of recombinant viruses, were performed as previously described<sup>[4]</sup>. The concentration unit of scAAV2 vector is vg/mL (vector genome per milliliter).

Recombinant lentivirus (LV) vectors encoding either GFP alone or GFP and C3 together, were prepared by the Beijing LKL Gene Company (Beijing, China), as previously described<sup>[6,9,17]</sup>. Expressions from these vectors were driven by CMV promoter (LV-CMV-C3-GFP; LV-CMV-GFP). The

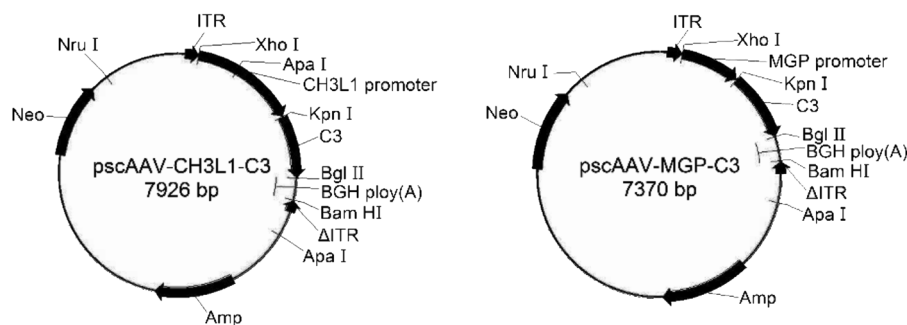


**Figure 1** Detailed structure of the representative self-complementary AAV2 vectors pscAAV: Self-complementary AAV plasmid; MGP: Matrix gla protein promoter; Ch3L1: Chitinase 3-like 1 promoter; C3: C3 transferase; Neo: Neomycin; Amp: Ampicillin; ITR: Inverted terminal repeat; BGH poly(A): Bovine growth hormone polyadenylation signal. Restriction enzyme sites: NruI, XhoI, KpnI, Bgl II, Bam HI, and Apa I.

**Table 1** Group assignments and summary of transduction conditions for the *in vitro* experiments

Trial	Culture plate	CN, cells/well	MV, mL/well	Group (scAAV2-mediated gene expression)		Titer, vg/mL	VV, $\mu$ L	Dose, vg	MOI
				Promoter	Gene				
1	24-well	$1 \times 10^5$	1	CMV	C3	$5 \times 10^{10}$	10	$5 \times 10^8$	$5 \times 10^3$
				eMGP	C3	$3.96 \times 10^{10}$	12.5	$5 \times 10^8$	$5 \times 10^3$
				MGP	C3	$8.28 \times 10^{10}$	5	$5 \times 10^8$	$5 \times 10^3$
				Ch3L1	C3	$6 \times 10^{10}$	8.5	$5 \times 10^8$	$5 \times 10^3$
2	24-well	$1 \times 10^5$	1	CMV	C3	$5 \times 10^{11}$	10	$5 \times 10^9$	$5 \times 10^4$
				eMGP	C3	$3.96 \times 10^{11}$	12.5	$5 \times 10^9$	$5 \times 10^4$
				MGP	C3	$8.28 \times 10^{11}$	6	$5 \times 10^9$	$5 \times 10^4$
				CMV	eGFP	$5 \times 10^{11}$	2	$1 \times 10^9$	$1 \times 10^4$
				CAG	eGFP	$2.5 \times 10^{11}$	4	$1 \times 10^9$	$1 \times 10^4$
3	6-well	$6 \times 10^5$	2	CMV	C3	$2.37 \times 10^{13}$	7	$1.66 \times 10^{11}$	$2.77 \times 10^5$
				MGP	C3	$1.17 \times 10^{14}$	7	$8.19 \times 10^{11}$	$1.37 \times 10^6$
				eMGP	C3	$1.26 \times 10^{14}$	6.5	$8.19 \times 10^{11}$	$1.37 \times 10^6$

CN: Cell numbers per well in culture plate; MV: Medium volume per well; vg/mL: Vector genome per milliliter; VV: Virus volume; MOI: Multiplicities of infection; scAAV2: Self-complementary adeno-associated virus 2; CMV: Cytomegalovirus promoter; CAG: A combination of chicken beta-actin promoter and cytomegalovirus immediate-early enhancer; MGP: Matrix gla protein promoter; eMGP: Enhanced MGP promoter; Ch3L1: Chitinase 3-like 1 promoter; C3: C3 transferase; eGFP: Enhanced green fluorescent protein.

concentration unit of LV vector is TU/mL (transducing units per milliliter).

**Cell Culture and Treatments** Primary human TM cells (ScienCell Research Laboratories, Inc., Carlsbad, CA, USA) were cultured in TM cell medium (TMCM; ScienCell Research Laboratories, Inc.) at 37°C in 5% CO<sub>2</sub>, as previously described<sup>[4,6,9]</sup>.

Group assignments and summary of transducing conditions are described in Table 1. Cells of passages 4 to 5 were transduced with several multiplicities of infections (MOIs) of the scAAV2-CMV-C3, scAAV2-Ch3L1-C3, scAAV2-eMGP-C3 or scAAV2-MGP-C3 vectors. At 24, and 48h after treatment, cells were harvested and processed for subsequent analyses. Images of morphology and fluorescence were taken using an Olympus CKX53 inverted fluorescence microscope (Olympus, Tokyo, Japan).

**RNA Isolation and Real-Time Quantitative Polymerase Chain Reaction Analysis** Real-time quantitative polymerase

chain reaction assays were performed as described previously with some modifications<sup>[9]</sup>. Glyceraldehyde-3-phosphate dehydrogenase (GAPDH) was used as the reference gene. The relative expression for each mRNA was calculated using the expression  $2^{-\Delta\Delta Ct}$  method. The specific gene products were amplified using the following primer pairs: C3-forward, 5'-TA CAAATATCGACCAGGCAAAGGCA-3'; C3-reverse, 5'-GC CCTTGGCCACCTTAAACTTTGTG-3'; RhoA-forward, 5'-GGATCTTCGGAATGATGAGCA-3'; RhoA-reverse, 5'-TGTTTGGCCATATCTCTGCCTTCT-3'; ROCK-2-forward, 5'-AAGTGGGTTAGTCGGTTG-3'; ROCK-2-reverse, 5'-GGCAGTTAGCTAGGTTTGTG-3'; GAPDH-forward, 5'-ACCACAGTCCATGCCATCAC-3'; GAPDH-reverse, 5'-TCCACCACCTGTTGCTGTA-3'.

**Western Blot Analysis** Transduced cells were rinsed with 1×Dulbecco's phosphate-buffered saline (PBS) and incubated in a cold radio immunoprecipitation assay (RIPA) lysis buffer (CWBio, Beijing, China) containing protease/

phosphatase inhibitor cocktail (Cell Signaling Technology, Danvers, MA, USA) on ice for 20min, and then clarified by centrifugation (16 000 g ×10min at 4°C). The protein concentrations were determined using the bicinchoninic acid (BCA) protein quantification kit (Yeasen Biotechnology Co., Ltd., Shanghai, China). A 4%-20% precast gel (Solarbio Science and Technology, Beijing, China) was loaded with 10 µg of protein lysate per lane, electrophoresed, and transferred to a commercial polyvinylidene fluoride membrane (Merck Millipore, Burlington, MA, USA). Membranes were blocked in a 5% non-fat dry milk in Tris-buffered saline and Tween-20 at room temperature for 1h. Membranes were incubated with primary antibodies against RhoA (#2117, rabbit monoclonal antibody, 1:1000; Cell Signaling Technology, Danvers, MA, USA), fibronectin (ab6328, Mouse monoclonal antibody, 1:1000; Abcam, Cambridge, MA, USA) or GAPDH (AF5718, goat polyclonal antibody, 1 µg/mL; R&D Systems, Minneapolis, MN, USA) at 4°C overnight. Immunostained membranes were then incubated with the horseradish peroxidase (HRP)-conjugated goat anti-rabbit IgG (1:10 000, ZSGB-Bio, Beijing, China), HRP-conjugated goat anti-mouse IgG (1:20 000, ZSGB-Bio) or HRP-conjugated rabbit anti-goat IgG secondary antibodies (1:20 000, ZSGB-Bio) at room temperature for 1h. Immunostained proteins were exposed with a Fluor ChemE (Cat. No.92-14860-00, ProteinSimple, San Jose, CA, USA). The signal densitometry was carried out by Image J software and normalized to the GAPDH protein in each lane (group).

**Actin Labeling and Immunocytochemistry** The human TM cells grown on climbing slices were washed with 1×Dulbecco's PBS and immersed in 4% paraformaldehyde (prepared from 8% paraformaldehyde stock solution in pure water; Solarbio Science and Technology) for 15min at 37°C with a water bath. Actin analyses were performed with Rhodamine-phalloidin (Cytoskeleton, Inc., Denver, CO, USA) staining as described previously<sup>[4,6,9]</sup>. Fixed cells were also permeabilized with 0.5% Triton X-100 in PBS (Wuhan Servicebio Co., Ltd., Wuhan, China) for 30min at 37°C with a water bath, blocked with 10% goat serum (Solarbio Science and Technology) in PBS for 1h at 37°C with a water bath, and subsequently incubated overnight at 4°C in the presence of a 1:200 dilution of mouse monoclonal anti-fibronectin antibody (ab6328; Abcam). Following washes with 1×PBS, immunostained cells were incubated with for 1h at 37°C (water bath) with a 1:450 dilution of AlexaFluor 594-conjugated goat anti-mouse IgG secondary antibody (A-11032; Invitrogen, Carlsbad, CA, USA). After washing with 1×PBS, nuclei were counterstained with Fluoroshield containing DAPI (4',6'-diamino-2-phenylindole, Sigma-Aldrich Corp., St. Louis, MO, USA). The labeled cells were captured using an Olympus CKX53 inverted fluorescence microscope (Olympus).

**Table 2 Summary of viral vector injections for animal study**

Trial	Group (injected vector)	Titer, particles/mL <sup>a</sup>	Volume, µL	Dose, particles <sup>a</sup>
1	scAAV2-Ch3L1-C3	6×10 <sup>10</sup>	5	3×10 <sup>8</sup>
	scAAV2-eMGP-C3	6×10 <sup>10</sup>	5	3×10 <sup>8</sup>
	LV-CMV-C3-GFP	5×10 <sup>8</sup>	5	2.5×10 <sup>6</sup>
	scAAV2-CAG-eGFP	6×10 <sup>10</sup>	5	3×10 <sup>8</sup>
	LV-CMV-GFP	5×10 <sup>8</sup>	5	2.5×10 <sup>6</sup>
2	scAAV2-CMV-C3	2.37×10 <sup>13</sup>	4	9.48×10 <sup>10</sup>
	scAAV2-MGP-C3	1.17×10 <sup>14</sup>	4	4.68×10 <sup>11</sup>
	scAAV2-eMGP-C3	1.26×10 <sup>14</sup>	3.7	4.68×10 <sup>11</sup>

<sup>a</sup>The units of vg/mL (vector genome per milliliter) in scAAV2 vector and TU/mL (transducing units per milliliter) in LV vector. scAAV2: Self-complementary AAV2; LV: Lentivirus vector; CMV: Cytomegalovirus promoter; CAG: A combination of chicken beta-actin promoter and cytomegalovirus immediate-early enhancer; MGP: Matrix gla protein promoter; eMGP: Enhanced MGP promoter; Ch3L1: Chitinase 3-like 1 promoter; C3: C3 transferase; eGFP: Enhanced green fluorescent protein.

**Animals** Sprague-Dawley rats weighing 200 to 240 g were purchased from Charles River Laboratory Animal Technology Company (Beijing, China). Rats were fed with a standard diet, unlimited water and housed in a room which remained at 22°C, 55% humidity, and 12-h cycle lighting.

**Viral Delivery to the Anterior Segment** Rats were anesthetized with 10% chloral hydrate (0.4 mL/100 g body weight; Sigma-Aldrich) given intraperitoneally. Intracameral injections were conducted as described previously, with some modifications<sup>[6]</sup>. Viral suspensions were delivered to one eye of each rat using a Hamilton glass syringe (10 µL volume; 7803-05; Hamilton Corp., Reno, NV, USA) with a 33-gauge needle (7635-01; Hamilton Corp.). Side of injection was randomized. The noninjected rats (both eyes) were used as blank control group. The grouping details and volume, titer and others of injection were summarized in Table 2.

**Clinical Examination** Eyes were examined using a slit lamp biomicroscope (S350, Shanghai MediWorks Precision Instruments Co., Ltd., Hangzhou, China) with an attached camera (EOS 600D, Canon, Inc., Tokyo, Japan).

**In Vivo Imaging of Green Fluorescence in the Anterior Segments** The fluorescent image system of a Micron IV Retinal Imaging Microscope (Phoenix Research Lab., Pleasanton, CA, USA) was used to examine the findings of green fluorescence in anterior segments as previously described<sup>[4,6,9]</sup>.

**Intraocular Pressure Measurement** IOP readings of the conscious rats were measured using the TonoLab rebound tonometer (Icare, Finland, Espoo, Finland) as previously described<sup>[6]</sup>. Measurements were taken at the same time of the day between 2–4 p.m. on day 0 (before injection), day 3, 7, 14 and 21.

**Eye Extraction and Histopathological Analysis** Eyeballs were enucleated from rats following sacrifice and fixed in a formaldehyde, acetic acid, and saline fixative (Wuhan Servicebio Co., Ltd., Wuhan, China). They were imbedded with paraffin, cut in 4- $\mu$ m sections, and stained with hematoxylin and eosin. Digital images were acquired by an Olympus CKX53 inverted fluorescence microscope (Olympus).

**Statistical Analysis** Statistics was done using SPSS (statistical product and service solutions) 18 software (IBM-SPSS, Chicago, IL, USA). Comparisons between two groups were analyzed using two-tailed paired Student's *t*-test. Comparisons of multiple groups were performed using one-way analysis of variance. *P*-values of <0.05 were considered statistically significant. Data are presented as mean $\pm$ standard error (SE).

## RESULTS

**Dose-effect Relationship at 24h Post Vector Delivery in Cultured Human TM cells** Human TM cells were transduced with C3-expressing scAAV2 vectors to evaluate the effects of C3 expression on cell morphology, actin cytoskeleton and its associated cellular adhesions. The expression and effects of C3 can also be evaluated as a "reporter gene" since C3 induced those changes are very sensitive and obvious. These C3-expressing scAAV2 vectors were driven by CMV, Ch3L1, eMGP and MGP promoter, respectively. The scAAV2 encoding eGFP gene was driven by CMV and CAG promoter, respectively.

Figure 2 showed the effects of C3 expression on the human TM cells after 24h treatment with different scAAV2 vectors at MOI of  $5\times 10^3$ ,  $5\times 10^4$ ,  $2.77\times 10^5$  or  $1.37\times 10^6$ .

At the MOI of  $5\times 10^3$ , human TM cells transduced with scAAV2-CMV-C3 or scAAV2-Ch3L1-C3 was either elongated or rounded up (Figure 2A). In these two groups, significant expression of C3 mRNA level was detected, a consequent decrease in ROCK-2 mRNA and a modest increase in RhoA mRNA were also observed (Figure 2B). Furthermore, there was disruption of the actin cytoskeleton and reduced positive immunofluorescent staining of fibronectin in human TM cells treated with scAAV2-CMV-C3 or scAAV2-Ch3L1-C3 (Figure 3). In contrast, the treatment of scAAV2-eMGP-C3 or scAAV2-MGP-C3 did not induce these effects in human TM cells as described above (Figures 2A, 2B, and 3).

When the MOI was increased to  $5\times 10^4$  (Figure 2A), the scAAV2-eMGP-C3-treated cells started to show signs of cell contraction, transcription of C3 mRNA, and significant decreases of ROCK-2 (Figure 2A, 2B). Moreover, the RhoA protein level was significantly decreased (Figure 2C), while RhoA mRNA level was slightly increased in the scAAV2-eMGP-C3-treated cells (Figure 2B). This discrepancy was similar to that described above and indicated a possible

feedback upregulation of the RhoA mRNA levels in response to the inhibition (and/or reduced levels) of RhoA protein by C3 expression. The morphological changes (Figure 2A) and the decrease of ROCK-2 mRNA level (Figure 2B) were more pronounced in the cells treated with scAAV2-CMV-C3. The protein expression of RhoA and fibronectin were significantly decreased in the scAAV2-CMV-C3-treated cells, and these changes were more significant than those in the scAAV2-eMGP-C3-treated cells (Figure 2C). In the scAAV2-MGP-C3-treated cells, although the transcript of C3 mRNA was present, the changes above were still not observed (Figure 2A-2C).

Since the effects were very weak in the cells treated with scAAV2-eMGP-C3 at an MOI of  $5\times 10^4$ , we selected a MOI of  $1.37\times 10^6$  for further transduction. As shown in Figure 2D, the C3 expression-induced effects became more obvious in the cells after treatment of scAAV2-eMGP-C3 at MOI of  $1.37\times 10^6$ . When the MOI was increased to  $1.37\times 10^6$ , contraction of cells treated with scAAV2-MGP-C3 started to occur at 24h (Figure 2D). Significant reductions of protein levels in RhoA and fibronectin were also found in the scAAV2-MGP-C3-treated cells, but weaker than that in scAAV2-eMGP-C3-treated cells (Figure 2E). Meanwhile, a large number of floating cells were observed in the human TM cells treated with a MOI of  $2.77\times 10^5$  of scAAV2-CMV-C3. This may due to the excessive cell contraction and substantial reduction of the extracellular matrix, and was rare in both groups of cells described above.

**In Vitro Fluorescent Signal of the Reporter Protein in Human TM cells Following Vector Transduction** For the *in vitro* transduction experiments in human TM cells, the scAAV2-CAG-eGFP and scAAV2-CMV-eGFP vectors were used as controls (Figure 4). At 24h post-transduction, the scAAV2-CAG-eGFP-transduced cells revealed higher reporter gene signal (integrated optical density) than that in the scAAV2-CMV-eGFP-transduced cells. When compared to the blank control, no significant changes of cell morphology, C3 mRNA and ROCK-2 mRNA, were found in cells transduced with either scAAV2-CAG-eGFP or scAAV2-CMV-eGFP. This result confirmed that effects of Rho/ROCK pathway inhibition were not induced by scAAV2 itself or scAAV2-mediated promoter expression, but rather the scAAV2-mediated C3 expression.

**In vivo Fluorescent Signal of the Reporter Protein in Anterior Segment Following Vector Delivery** Previous animal studies by ourselves and others have demonstrated that scAAV2 vectors containing the transgenes driven by CMV promoter had a high tropism for the cells of the TM, iris and corneal endothelium<sup>[4,18]</sup>, while lentiviral vectors almost exclusively on the TM<sup>[9,19]</sup>.

For low-dose experiments, rat eyes were injected intracamerally with an equal dose ( $3\times 10^8$  vg) of scAAV2-Ch3L1-C3, scAAV2-eMGP-C3 and scAAV2-CAG-eGFP, respectively

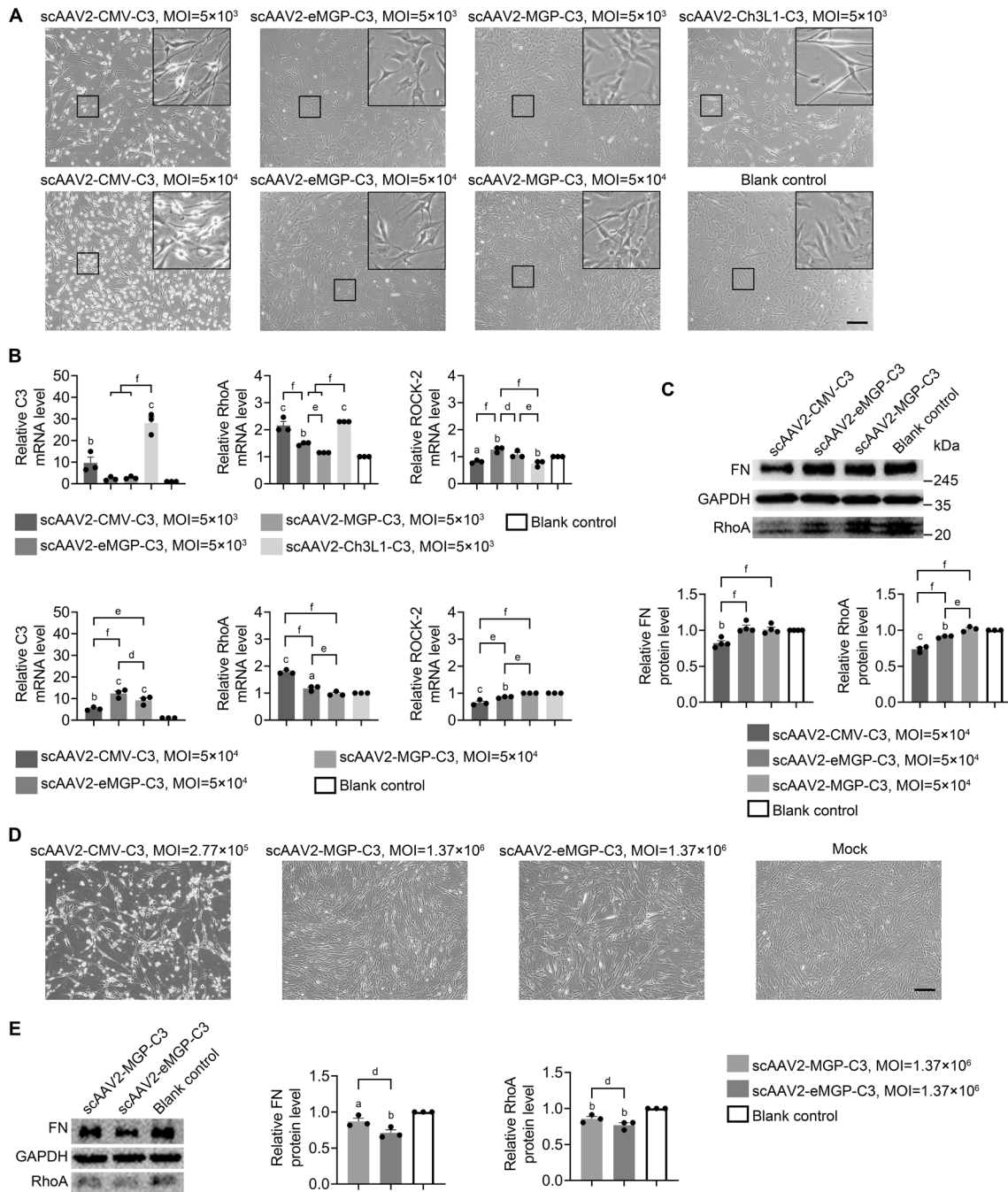


**Figure 2 C3 transferase (C3) expression-induced changes in the human trabecular meshwork (TM) cells at 24h post-transduction** C3-expressing self-complementary AAV2 (scAAV2) vectors were driven by cytomegaloviruses (scAAV2-CMV-C3), chitinase 3-like 1 (scAAV2-Ch3L1-C3), enhanced matrix gla protein (MGP; scAAV2-eMGP-C3) and MGP (scAAV2-MGP-C3) promoter, respectively. Each vector was delivered to the cells at gradient multiplicities of infections (MOIs). A, D: Morphological changes. The boxed region in each image was enlarged in the inset to show the typical morphologies induced by C3 expression. Scale bar=200  $\mu$ m. B: Changes of mRNA levels in C3, Rho GTPase A (RhoA) and Rho-associated kinase 2 (ROCK-2). C, E: Changes of protein levels in RhoA and fibronectin (FN). Result of each group was normalized to reference protein glyceraldehyde-3-phosphate dehydrogenase (GAPDH) or mRNA GAPDH, and this value was further standardized to that value of blank control group. Error bars show standard error of mean (SEM), and the significance of difference was calculated using one-way analysis of variance. <sup>a</sup> $P$ <0.05, <sup>b</sup> $P$ <0.01, <sup>c</sup> $P$ <0.001 versus baseline; <sup>d</sup> $P$ <0.05, <sup>e</sup> $P$ <0.01, and <sup>f</sup> $P$ <0.001.

(Table 2). As controls, LV-CMV-C3-GFP and LV-CMV-GFP were injected separately into rat eyes at a same dose of  $2.5 \times 10^6$  TU (Table 2). Meanwhile, a high-dose experiment was also performed to further confirm the initiation capacity of MGP promoter. Rat eyes were injected intracamerally with an

equal dose ( $4.68 \times 10^{11}$  vg) of scAAV2-MGP-C3 and scAAV2-eMGP-C3, respectively (Table 2). Given the high initiation capacity of CMV promoter in the TM cells, a dose ( $9.48 \times 10^{10}$  vg) of scAAV2-CMV-C3 was administrated to the rat eyes as a control. As shown in Figure 4, the features of the fluorescence

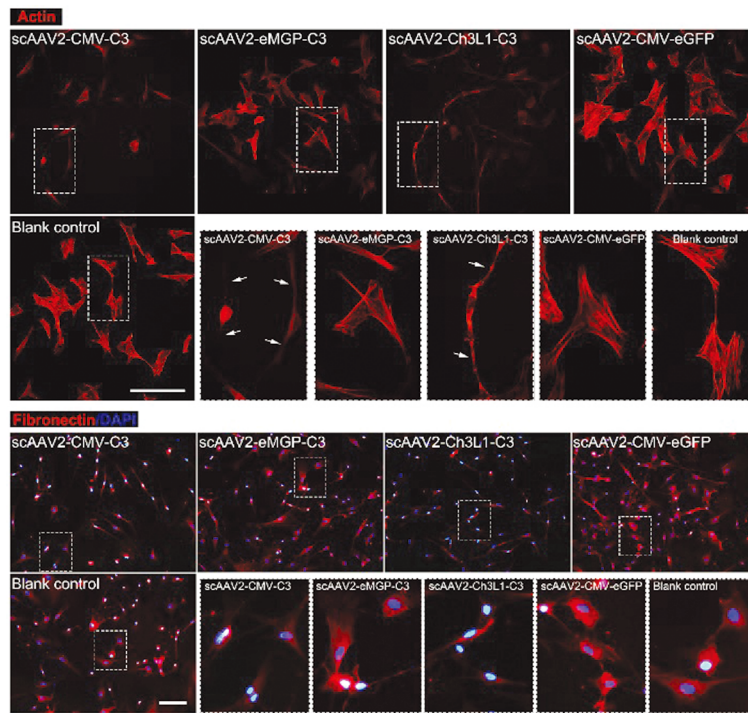


**Figure 3 Actin labeling and fibronectin immunofluorescence staining at 24h post-transduction** The human trabecular meshwork cells were transduced with scAAV2-CMV-C3, scAAV2-Ch3L1-C3, scAAV2-eMGP-C3, and scAAV2-CMV-eGFP, respectively. All vectors were delivered to the cells at multiplicities of infection of  $5 \times 10^3$ . Typical cells were outlined and enlarged in dashed boxes. Nuclei were counterstained with 4',6-diamidino-2-phenylindole (DAPI). Arrows indicate the contracted cell bodies. scAAV2: Self-complementary AAV2; CMV: Cytomegalovirus promoter; MGP: Matrix gla protein promoter; eMGP: Enhanced MGP promoter; Ch3L1: Chitinase 3-like 1 promoter; C3: C3 transferase; eGFP: Enhanced green fluorescent protein. Scale bar = 200  $\mu\text{m}$ .

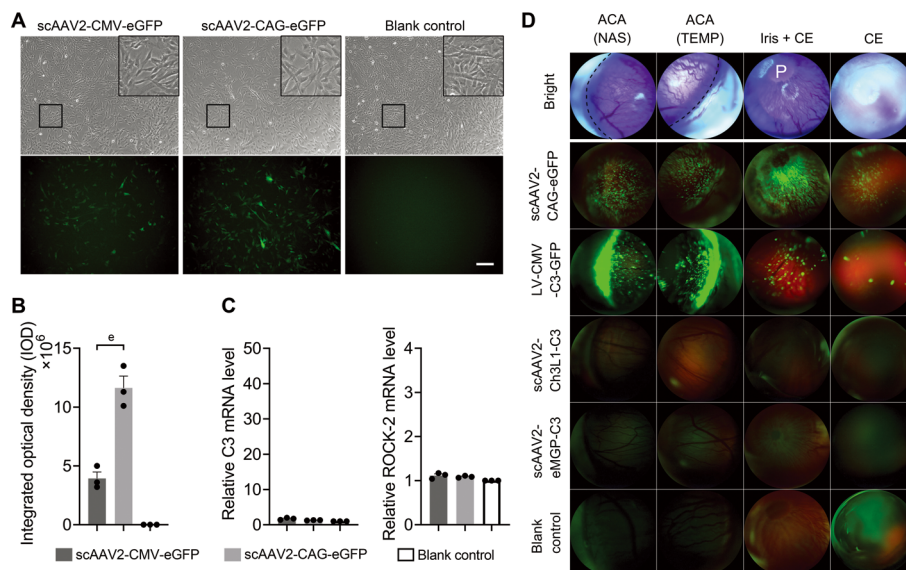


**Figure 4 In vitro and in vivo analyses after treatments of fluorescent protein-expressing vectors** A-C: Changes in cell morphology, enhanced green fluorescent protein (eGFP) expression and mRNA levels of C3 transferase (C3) and Rho-associated kinase 2 (ROCK-2) in human trabecular meshwork (TM) cells. All vectors were delivered to the cells at multiplicities of infection of  $1 \times 10^4$ . A: Cell morphology and green fluorescence. Scale bar = 200  $\mu\text{m}$ . B: Intensity of green fluorescence was calculated and presented as integrated optical density (IOD). C: mRNA levels of C3 and ROCK-2. Error bars show standard error of mean, and the significance difference was calculated using one-way analysis of variance (ANOVA).  $^e P < 0.01$ . D: *In vivo* expression of green fluorescent protein in the anterior segment tissues of rats at 15d post-injection. The black dashed lines indicate the position of the TM. To examine corneal fluorescence, 0.5% tropicamide/phenylephrine (Mydrin P; Santen Pharmaceutical Co., Ltd., Osaka, Japan) was used to dilate the pupil for avoiding the interference from the iris fluorescence. ACA: Anterior chamber angle; NAS: Nasal side; TEMP: Temporal side; CE: Corneal endothelium; P: Pupil; scAAV2: Self-complementary AAV2; LV: Lentivirus vector; CMV: Cytomegalovirus promoter; CAG: A combination of chicken beta-actin promoter and cytomegalovirus immediate-early enhancer; eMGP: Enhanced matrix gla protein promoter; Ch3L1: Chitinase 3-like 1 promoter.

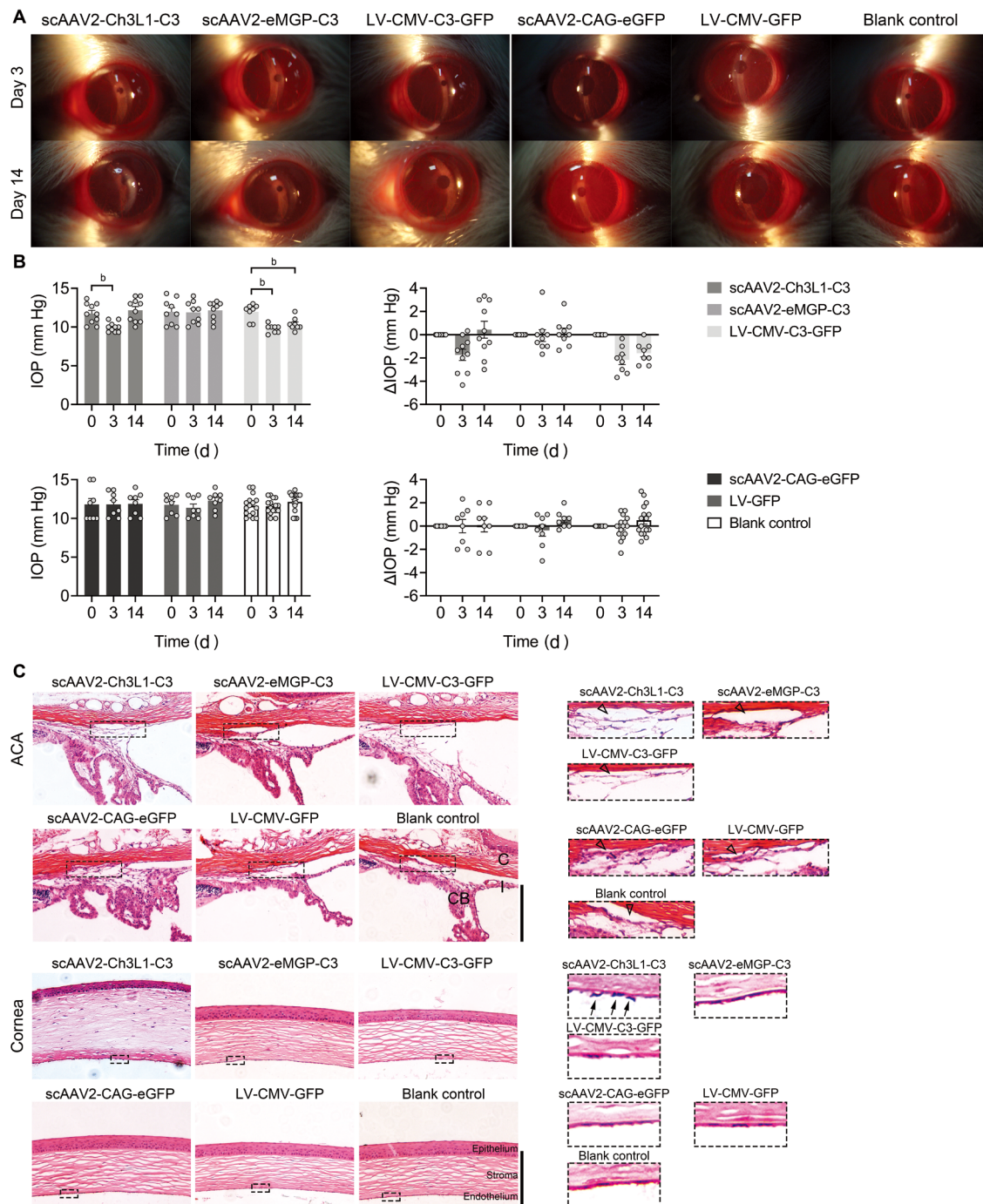


**Figure 5 Slit-lamp examination, intraocular pressure (IOP) response and histological analyses in rat eyes at different timepoints after low-dose vector injections** A: Representative images of anterior segment of eyes on day 3 and 14. B: IOP changes on day 0 (baseline), 3 and 14.  $\Delta$ IOP indicates the difference between IOP before and after transduction. Error bars show standard error of mean, and the significance difference was calculated using two-tailed paired *t*-test. <sup>b</sup>*P*<0.01. C: Representative images of hematoxylin and eosin-staining on anterior chamber angles (ACA) and central corneas on day 21. Trabecular meshwork (TM) and corneal endothelium were outlined and enlarged in dashed box. Hollow arrowheads indicate Schlemm's canal. Arrows indicate the cell contraction. I: Iris; CB: Ciliary body; scAAV2: Self-complementary AAV2; LV: Lentivirus vector; CMV: Cytomegalovirus promoter; CAG: A combination of chicken beta-actin promoter and cytomegalovirus immediate-early enhancer; eMGP: Enhanced matrix gla protein promoter; Ch3L1: Chitinase 3-like 1 promoter; C3: C3 transferase; eGFP: Enhanced green fluorescent protein. Scale bar =200  $\mu$ m.

distributions in rat eyes were very similar to that described above. The scAAV2-CAG-eGFP-injected eyes also exhibited obvious signals of green fluorescence in TM, iris, and corneal endothelium.

**Monitoring Reactions in the Anterior Segments** In the low-dose experiment (Figure 5A), none of the groups showed signs of opacity or inflammation at day 3. Subsequently, only the scAAV2-Ch3L1-C3 group exhibited variable degree of corneal



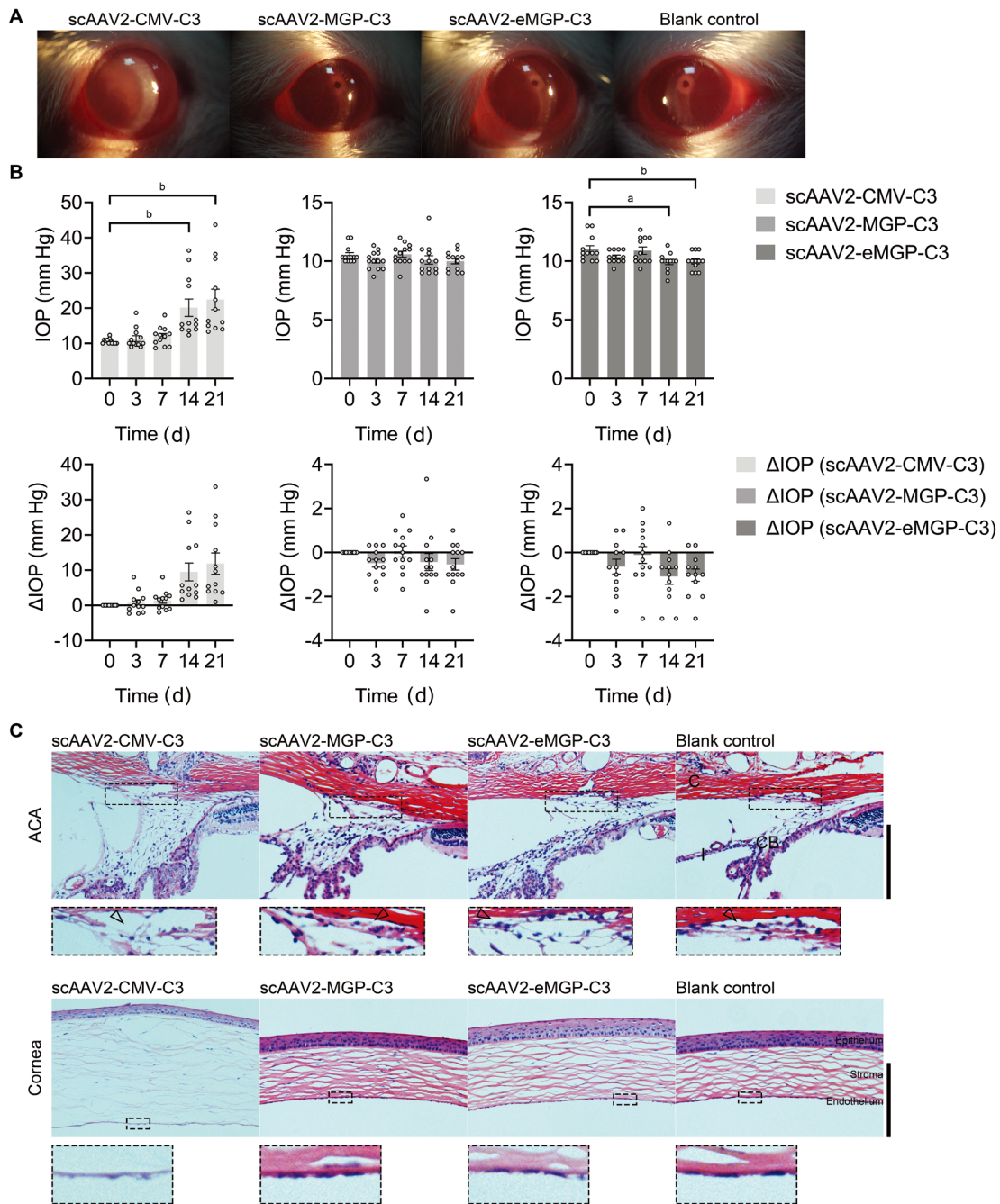


**Figure 6 Slit-lamp examination, intraocular pressure (IOP) response and histological analyses in rat eyes at different timepoints after high-dose vector injections** A: Representative images of anterior segment of eyes at 21d. B: IOP changes on day 0 (baseline), 3, 14, and 21. ΔIOP indicates the difference between IOP before and after transduction. Error bars show standard error of mean (SEM), and the significance difference was calculated using two-tailed paired *t*-test. <sup>a</sup>*P*<0.05, <sup>b</sup>*P*<0.01. C: Representative images of hematoxylin and eosin-staining at anterior chamber angles (ACA) and central corneas on day 21. Trabecular meshwork (TM) and corneal endothelium were outlined and enlarged in dashed box. Hollow arrowheads indicate Schlemm’s canal. C: Cornea; I: Iris; CB: Ciliary body; scAAV2: Self-complementary AAV2; CMV: Cytomegalovirus promoter; MGP: Matrix gla protein promoter; eMGP: Enhanced MGP promoter; C3: C3 transferase. Scale bar =200 μm.

edema at day 14 post-injection. In the high-dose experiment (Figure 6A), obvious corneal edema was found in the scAAV2-CMV-C3 group as early as day 3 (data not shown), and markedly aggravated at day 21 post-injection. However, no abnormalities were observed in scAAV2-MGP-C3 and scAAV2-eMGP-C3 groups. No inflammation was observed in rat eyes post-injection.

**Intraocular Pressure Changes in Rat Eyes** In the low-dose experiment (Figure 5B), the pretreatment IOP (baseline) was 11.73±0.42, 11.96±0.55, and 11.96±0.37 mm Hg in eyes to be injected with scAAV2-Ch3L1-C3 (*n*=10), scAAV2-eMGP-C3 (*n*=9) and LV-CMV-C3-GFP (*n*=8), respectively. At day 3 post-injection, the eyes injected with scAAV2-Ch3L1-C3 or LV-CMV-C3-GFP showed a significant IOP decrease, when

compared to baseline, with a mean IOP reduction ( $\Delta$ IOP) of  $1.73 \pm 0.48$  mm Hg in scAAV2-Ch3L1-C3 group or  $2.17 \pm 0.41$  mm Hg in LV-CMV-C3-GFP group. At day 14 post-injection, the  $\Delta$ IOP of LV-CMV-C3-GFP-injected eyes was  $1.58 \pm 0.33$  mm Hg. However, corneal edema in scAAV2-Ch3L1-C3-injected eyes caused a higher measured value of IOP ( $12.17 \pm 0.47$  mm Hg) and a lower calculated value of  $\Delta$ IOP ( $0.43 \pm 0.73$  mm Hg). This was consistent with our and other previous observations that the corneal thickening can result in higher measured IOP values<sup>[4,20-22]</sup>. The IOP did not present significant changes in the scAAV2-eMGP-C3-injected eyes at day 3 and 14 post-injection. The pretreatment IOP (baseline) was  $11.79 \pm 0.78$  and  $11.75 \pm 0.44$  mm Hg in eyes to be injected with scAAV2-CAG-eGFP ( $n=8$ ) and LV-CMV-GFP ( $n=8$ ), respectively. No significant IOP changes were observed in these two groups at day 3 and 14 post-injection.

In the high-dose experiment (Figure 6B), the pretreatment IOP (baseline) was  $10.61 \pm 0.22$ ,  $10.54 \pm 0.19$ , and  $11.00 \pm 0.31$  mm Hg in eyes to be injected with scAAV2-CMV-C3 ( $n=12$ ), scAAV2-MGP-C3 ( $n=13$ ) and scAAV2-eMGP-C3 ( $n=12$ ), respectively. At day 14 post-injection, a significant IOP change began to be detected in the scAAV2-eMGP-C3 group, when compared to the baseline, with a  $\Delta$ IOP of  $1.08 \pm 0.36$  mm Hg. Since obvious corneal edema was occurred as early as day 3, a trend toward higher measured values of IOP was detected on the scAAV2-CMV-C3-injected eyes, and began to be statistically significant at day 14. In the scAAV2-MGP-C3 group, there were no significant IOP changes compared with the baseline.

**Hematoxylin and Eosin Staining of Rat Eye Anterior Segment** In the low-dose experiment (Figure 5C), little difference in the structure of the TM tissues was observed among the blank control eyes and the eyes after treatment of scAAV2-eMGP-C3, scAAV2-CAG-eGFP, and LV-CMV-GFP, respectively. In contrast, the anterior segments transduced with scAAV2-Ch3L1-C3 or LV-CMV-C3-GFP exhibited C3-induced morphological changes in the TM including loose stroma and reduced cellularity. In the high-dose experiment (Figure 6C), morphological differences in the TM were not apparent between the scAAV2-MGP-C3 group and blank control. C3-induced TM morphological characteristics were observed in scAAV2-CMV-C3 group, and began to be visualized in the scAAV2-eMGP-C3 groups.

As a result of actin-associated endothelial barrier disruption induced by C3 expression, the scAAV2-Ch3L1-C3-transduced and scAAV2-CMV-C3-transduced eyes showed an edematous corneal stroma with blurring borders of collagen fiber, and the contracted endothelium was loosely connected to the base membrane (Figures 5C and 6C). No abnormalities were found in the other groups (Figures 5C and 6C), indicating the vectors themselves were not able to cause obvious changes in corneal

endothelium.

## DISCUSSION

Glaucoma remains the leading cause of irreversible blindness in the world. Currently, almost all the modalities of management are focused on reduction of IOP, the major risk factor of the disease. However, the current medical lowering IOP strategies exhibit a number of problems. As an example, patients usually require more than 1 medication on a daily basis over time in order to lower the IOP, and may have hard time with adherence to multiple topical drop regimens. In addition, there are a number of side effects related to these medications. Therefore, much attention has been given to development of gene therapy, with a hope to lower the IOP at a relatively long duration after single treatment.

For IOP-lowering gene therapy, it is critical to use vectors capable of targeting TM, the conventional aqueous humor drainage pathway which account for major outflow resistance in human, when administered to anterior chamber. However, other than effectiveness of transgene expression, the specificity of gene targeting remains the major challenge. Previous *in vivo* studies<sup>[7,11,18,23]</sup> showed that intracameral delivery of the scAAV2 vectors (containing CMV promoter in most of these studies) transduced not only the TM, but also the corneal endothelium and iris without inducing an inflammatory response and other abnormalities. Our current and previous results were in agreement with these findings, and confirmed the scAAV2 vector possessed a broad-spectrum transduction of anterior chamber tissues in mice, rats and monkeys<sup>[4]</sup>. Moreover, in comparison with LV vector-mediated C3 expression system, scAAV2 vector-mediated C3 expression yielded a longer-lasting IOP-lowering effect (at least 4mo in LV-C3 vector versus at least 10mo in scAAV2-C3 vector)<sup>[49]</sup>. Therefore, as long as the duration of effectiveness is considered, scAAV2 vector may hold greater potential in application of glaucoma gene therapy for glaucoma in the future.

One critical challenge for bringing scAAV2-mediated C3 expression system into clinical trials involves equipping both significant protein expression (efficacy) and high TM-specificity (safety). The choice of the proper or specific promoter to initiate transgene expression in the TM remains a key issue in glaucoma gene therapy. Previous studies using the recombinant adenoviruses containing the *LacZ* gene driven by either MGP promoter or Ch3L1 promoter resulted in high transgene expression levels and specificity in the TM of perfused human anterior segments<sup>[13-15]</sup>. In the current study, the Ch3L1 promoter was similar to the CMV promoter in its ability to drive C3 protein expression in the TM, both *in vivo* and *in vitro*, but was far superior to the eMGP and MGP promoters. Furthermore, the Ch3L1 promoter did not change the tissue tropism of scAAV2 vector, and initiated C3

gene expression not only in the TM but also in the corneal endothelium. The reason why our findings are different from previous studies is not clear, but several factors might be involved. First, different viral vectors were used. When the CMV promoter was employed, the adenoviral vector had high tropism in several types of the anterior chamber tissues similar to the scAAV2 vector<sup>[24-25]</sup>. Interestingly, substituting CMV promoter for Ch3L1 promoter resulted in a lack of adenovirus-mediated transgene expression in the corneal endothelium, but failed to affect scAAV2-mediated transgene expression in these cells, as described in the previous<sup>[15]</sup> and current studies. As shown in the Figure 4, the CAG promoter was also selected for driving reporter gene (eGFP) in the scAAV2 vector and had no effect on the distribution of the fluorescence (eGFP expression) in the anterior chamber post-injection. A possible explanation for these differences is that promoter such as CMV, Ch3L1 or CAG had different effects on the patterns of transgene expression mediated by different viral vector genes in the anterior chamber tissues. Second, different experimental animals were used. The differences in anatomical spaces of the anterior chamber and/or aqueous humor dynamics may affect the transduction pattern of viral vector. Since volume and outflow facility of anterior chamber in human were about ten times higher than that in rat, the deliveries of viral particles to the outflow pathways were more efficient<sup>[25-28]</sup>. In other words, longer residence times of viral particles in anterior chamber may result in greater uptake by corneal endothelial cells or other cells. Furthermore, in the anterior chamber tissues, the Ch3L1 promoter preferentially expresses in the TM<sup>[15]</sup>, and is also detected in corneal endothelium when stimulated by fungal infection. This expression is regulated *via* antifungal innate immune responses in the cornea<sup>[29]</sup> indicating that the Ch3L1 promoter may be active in corneal endothelial cells under some conditions. Further studies are needed to ascertain whether Ch3L1 was expressed in the viral vector-transduced cornea without inflammation. These results may explain why transgene expression was detected in the corneal endothelium of rat eyes injected with the scAAV2-mediated C3 expression driven by Ch3L1 promoter, but not in that of human eyes injected with the adenovirus-mediated  $\beta$ -galactosidase expression driven by same promoter.

Previous reports have demonstrated abundant MGP expression not only in the TM but also in the corneal endothelium, which in turn initiated adenovirus-mediated  $\beta$ -galactosidase expression efficiently in the TM cells<sup>[13,30]</sup>. However, our results showed that the transgene expression was very inefficient in the TM cells transduced with scAAV2 vectors controlled by either MGP promoter or eMGP promoter. The reason for this difference was unclear and may also be related to the different viral vectors used.

Fibronectin fibrils are a major component of the extracellular matrix in the TM, and its abnormal accumulation is thought to increase IOP through several complex pathways<sup>[31-32]</sup>. The Rho/ROCK pathway play an important role in the IOP modulation, as demonstrated by the significant increase of outflow facility and reduction of IOP after treatment of its inhibitors<sup>[4,6,9,33-34]</sup>. Fujimoto *et al*<sup>[35]</sup> showed that a selective ROCK inhibitor blocked the increased fibronectin expression induced by dexamethasone in TM cells. RhoA is a major upstream signaling molecule of ROCK, and our results revealed that the C3-induced RhoA inhibition disrupted the actin cytoskeleton and reduced the fibronectin expression in the human TM cells. Thus, the C3 gene therapy may be effective to reduce IOP in eyes with steroid-induced ocular hypertension and glaucoma. In contrast to decreased levels of RhoA protein, significant transcription levels of RhoA gene (increased mRNA levels) were detected. Correspondingly, one of its downstream effectors, ROCK-2, showed reductions of mRNA levels as well. Similar discrepancies have also been reported in other studies<sup>[36-37]</sup> and could be due to a feedback autoregulation of signaling pathway in cells. Although the specific mechanism was unknown, at least in TM cells, decreased levels of RhoA protein were observed. This was likely caused by C3-induced RhoA inactivation which was accompanied by increased mRNA expression.

Currently, classic pressure-dependent rat models generated by a series of methods, including intracameral injection of microbead<sup>[38-40]</sup> or viscous agent<sup>[41-42]</sup>, laser photocoagulation of outflow pathway<sup>[38,43-44]</sup>, cautery of extraocular veins<sup>[45-46]</sup>, glucocorticoid induction<sup>[47-48]</sup>, transduction of the TM with glaucoma related genes<sup>[49-51]</sup>, or in combination with each other<sup>[52-53]</sup>, are widely used to understand the pathogenic mechanism of glaucoma, and regarded as relatively cost-efficient tools for developing potential glaucoma therapies. In this study, normal rats were used to evaluate initiation efficiencies of two TM-specific promoters in the scAAV2 vector. This was chosen because simpler methods may help to decrease some uncertainties during tissue-specific observations. Previous studies have reported that glaucoma with higher baseline IOP showed greater IOP reduction after IOP-lowering treatment<sup>[54-55]</sup>. Nonetheless, the initiation efficiency of scAAV2 vector-mediated gene expression initiated by MGP promoter in TM did exhibit a relatively weaker effect compared with the Ch3L1 promoter or the commonly used CMV promoter.

In summary, in scAAV2-transduced TM cells, the promoter-driven efficiency of Ch3L1 was close to that of CMV, but obviously higher than that of MGP. In the anterior chamber of rat eye, the transgene expression pattern of scAAV2 vector was presumably affected by MGP promoter, but not by Ch3L1 promoter. These findings would provide a useful reference

for improvement of specificity and safety in glaucoma gene therapy using scAAV2 vector.

#### ACKNOWLEDGEMENTS

The authors thank Mr. Aaron Kolb from University of Wisconsin-Madison for proofreading the manuscript.

**Foundations:** Supported by the National Natural Science Foundation of China (No.81900829; No.82070963); the Xiamen Medical and Health Guiding Project Fund Project (No.3502Z20214ZD1214); the Guangdong Basic and Applied Basic Research Foundation (No.2019A1515011234); the Science and Technology Innovation Committee of Shenzhen (No.JCYJ20210324125614039).

**Conflicts of Interest:** Tan JK, None; Xiao Y, None; Liu G, None; Huang LX, None; Ma WH, None; Xia Y, None; Wang XZ, None; Zhu XJ, None; Cai SP, None; Wu XB, None; Wang Y, None; Liu XY, None.

#### REFERENCES

- van Zyl T, Yan WJ, McAdams A, Peng YR, Shekhar K, Regev A, Juric D, Sanes JR. Cell atlas of aqueous humor outflow pathways in eyes of humans and four model species provides insight into glaucoma pathogenesis. *Proc Natl Acad Sci U S A* 2020;117(19):10339-10349.
- Gazzard G, Konstantakopoulou E, Garway-Heath D, Garg A, Vickerstaff V, Hunter R, Ambler G, Bunce C, Wormald R, Nathwani N, Barton K, Rubin G, Buszewicz M, Group LTS. Selective laser trabeculoplasty versus eye drops for first-line treatment of ocular hypertension and glaucoma (LiGHT): a multicentre randomised controlled trial. *Lancet* 2019;393(10180):1505-1516.
- Nettesheim A, Shim MS, Dixon A, Raychaudhuri U, Gong HY, Liton PB. Cathepsin B localizes in the caveolae and participates in the proteolytic cascade in trabecular meshwork cells. potential new drug target for the treatment of glaucoma. *J Clin Med* 2020;10(1):78.
- Tan JK, Wang XZ, Cai SP, He F, Zhang DR, Li DK, Zhu XJ, Zhou L, Fan N, Liu XY. C3 transferase-expressing scAAV2 transduces ocular anterior segment tissues and lowers intraocular pressure in mouse and monkey. *Mol Ther Methods Clin Dev* 2020;17:143-155.
- Kaufman PL. Deconstructing aqueous humor outflow - The last 50 years. *Exp Eye Res* 2020;197:108105.
- Tan JK, Fan N, Wang NL, Feng BK, Yang M, Liu G, Wang Y, Zhu XJ, Kaufman PL, Pang IH, Liu XY. Effects of lentivirus-mediated C3 expression on trabecular meshwork cells and intraocular pressure. *Invest Ophthalmol Vis Sci* 2018;59(12):4937-4944.
- Borrás T, Buie LK, Spiga MG. Inducible scAAV2.GRE.MMP1 lowers IOP long-term in a large animal model for steroid-induced glaucoma gene therapy. *Gene Ther* 2016;23(5):438-449.
- Qiao YS, Sun ZM, Tan C, Lai JY, Sun XH, Chen JY. Intracameral injection of AAV-DJ.COMP-ANG1 reduces the IOP of mice by reshaping the trabecular outflow pathway. *Invest Ophthalmol Vis Sci* 2022;63(13):15.
- Tan JK, Liu G, Zhu XJ, Wu ZJ, Wang NL, Zhou L, Zhang XG, Fan N, Liu XY. Lentiviral vector-mediated expression of exoenzyme C3 transferase lowers intraocular pressure in monkeys. *Mol Ther* 2019;27(7):1327-1338.
- Luna C, Parker M, Challa P, Gonzalez P. Long-term decrease of intraocular pressure in rats by viral delivery of miR-146a. *Transl Vis Sci Technol* 2021;10(8):14.
- Borrás T, Buie LK, Spiga MG, Carabana J. Prevention of nocturnal elevation of intraocular pressure by gene transfer of dominant-negative RhoA in rats. *JAMA Ophthalmol* 2015;133(2):182-190.
- Kumar S, Shah S, Tang HM, Smith M, Borrás T, Danias J. Tissue plasminogen activator in trabecular meshwork attenuates steroid induced outflow resistance in mice. *PLoS One* 2013;8(8):e72447.
- Gonzalez P, Epstein DL, Luna C, Liton PB. Characterization of free-floating spheres from human trabecular meshwork (HTM) cell culture *in vitro*. *Exp Eye Res* 2006;82(6):959-967.
- Gonzalez P, Caballero M, Liton PB, Stamer WD, Epstein DL. Expression analysis of the matrix GLA protein and VE-cadherin gene promoters in the outflow pathway. *Invest Ophthalmol Vis Sci* 2004;45(5):1389-1395.
- Liton PB, Liu XL, Stamer WD, Challa P, Epstein DL, Gonzalez P. Specific targeting of gene expression to a subset of human trabecular meshwork cells using the chitinase 3-like 1 promoter. *Invest Ophthalmol Vis Sci* 2005;46(1):183-190.
- Dong XY, Tian WH, Wang G, Dong ZY, Shen W, Zheng G, Wu XB, Xue JL, Wang Y, Chen JZ. Establishment of an AAV reverse infection-based array. *PLoS One* 2010;5(10):e13479.
- Tan JK, Liu G, Lan CL, Pang IH, Luo XL, Wu S, Fan N, Zhang JX, Wang NL, Liu XY. Lentiviral vector-mediated expression of C3 transferase attenuates retinal ischemia and reperfusion injury in rats. *Life Sci* 2021;272:119269.
- Buie LK, Rasmussen CA, Porterfield EC, Ramgolam VS, Choi VW, Markovic-Plese S, Samulski RJ, Kaufman PL, Borrás T. Self-complementary AAV virus (scAAV) safe and long-term gene transfer in the trabecular meshwork of living rats and monkeys. *Invest Ophthalmol Vis Sci* 2010;51(1):236-248.
- Barraza RA, Rasmussen CA, Loewen N, Cameron JD, Gabelt BT, Teo WL, Kaufman PL, Poeschla EM. Prolonged transgene expression with lentiviral vectors in the aqueous humor outflow pathway of nonhuman Primates. *Hum Gene Ther* 2009;20(3):191-200.
- von Spiessen L, Karck J, Rohn K, Meyer-Lindenberg A. Clinical comparison of the TonoVet(®) rebound tonometer and the Tono-Pen Vet(®) applanation tonometer in dogs and cats with ocular disease: glaucoma or corneal pathology. *Vet Ophthalmol* 2015;18(1):20-27.
- Martinez-de-la-Casa JM, Garcia-Feijoo J, Vico E, Fernandez-Vidal A, Benitez del Castillo JM, Wasfi M, Garcia-Sanchez J. Effect of corneal thickness on dynamic contour, rebound, and goldmann tonometry. *Ophthalmology* 2006;113(12):2156-2162.
- Dohadwala AA, Munger R, Damji KF. Positive correlation between Tono-pen intraocular pressure and central corneal thickness. *Ophthalmology* 1998;105(10):1849-1854.

- 23 Lee SH, Sim KS, Kim CY, Park TK. Transduction pattern of AAVs in the trabecular meshwork and anterior-segment structures in a rat model of ocular hypertension. *Mol Ther Methods Clin Dev* 2019;14:197-205.
- 24 Borrás T, Gabelt BT, Klintworth GK, Peterson JC, Kaufman PL. Non-invasive observation of repeated adenoviral GFP gene delivery to the anterior segment of the monkey eye *in vivo*. *J Gene Med* 2001;3(5):437-449.
- 25 Li G, Gonzalez P, Camras LJ, Navarro I, Qiu J, Challa P, Stamer WD. Optimizing gene transfer to conventional outflow cells in living mouse eyes. *Exp Eye Res* 2013;109:8-16.
- 26 Ficarrota KR, Bello SA, Mohamed YH, Passaglia CL. Aqueous humor dynamics of the brown-Norway rat. *Invest Ophthalmol Vis Sci* 2018;59(6):2529-2537.
- 27 Stankowska DL, Millar JC, Kodati B, Behera S, Chaphalkar RM, Nguyen T, Nguyen KT, Krishnamoorthy RR, Ellis DZ, Acharya S. Nanoencapsulated hybrid compound SA-2 with long-lasting intraocular pressure-lowering activity in rodent eyes. *Mol Vis* 2021;27:37-49.
- 28 Thomasy SM, Eaton JS, Timberlake MJ, Miller PE, Matsumoto S, Murphy CJ. Species differences in the geometry of the anterior segment differentially affect anterior chamber cell scoring systems in laboratory animals. *J Ocul Pharmacol Ther* 2016;32(1):28-37.
- 29 Gao N, Yu FS X. Chitinase 3-like 1 promotes candida albicans killing and preserves corneal structure and function by controlling host antifungal responses. *Infect Immun* 2015;83(10):4154-4164.
- 30 Sakai R, Kinouchi T, Kawamoto S, Dana MR, Hamamoto T, Tsuru T, Okubo K, Yamagami S. Construction of human corneal endothelial cDNA library and identification of novel active genes. *Invest Ophthalmol Vis Sci* 2002;43(6):1749-1756.
- 31 Filla MS, Faralli JA, Desikan H, Peotter JL, Wannow AC, Peters DM. Activation of  $\alpha\beta3$  integrin alters fibronectin fibril formation in human trabecular meshwork cells in a ROCK-independent manner. *Invest Ophthalmol Vis Sci* 2019;60(12):3897-3913.
- 32 Faralli JA, Filla MS, Peters DM. Role of fibronectin in primary open angle glaucoma. *Cells* 2019;8(12):1518.
- 33 Abbhi V, Piplani P. Rho-kinase (ROCK) inhibitors - A neuroprotective therapeutic paradigm with a focus on ocular utility. *Curr Med Chem* 2020;27(14):2222-2256.
- 34 Berrino E, Supuran CT. Rho-kinase inhibitors in the management of glaucoma. *Expert Opin Ther Pat* 2019;29(10):817-827.
- 35 Fujimoto T, Inoue T, Kameda T, Kasaoka N, Inoue-Mochita M, Tsuboi N, Tanihara H. Erratum. involvement of RhoA/rho-associated kinase signal transduction pathway in dexamethasone-induced alterations in aqueous outflow. *Invest Ophthalmol Vis Sci* 2015;56(3):1593.
- 36 Al Labban D, Jo SH, Ostano P, Saglietti C, Bongiovanni M, Panizzon R, Dotto GP. Notch-effector CSL promotes squamous cell carcinoma by repressing histone demethylase KDM6B. *J Clin Invest* 2018;128(6):2581-2599.
- 37 Shivakumar M, Subbanna S, Joshi V, Basavarajappa BS. Postnatal ethanol exposure activates HDAC-mediated histone deacetylation, impairs synaptic plasticity gene expression and behavior in mice. *Int J Neuropsychopharmacol* 2020;23(5):324-338.
- 38 Colbert MK, Ho LC, van der Merwe Y, Yang XL, McLellan GJ, Hurley SA, Field AS, Yun HM, Du YQ, Conner IP, Parra C, Faiq MA, Fingert JH, Wollstein G, Schuman JS, Chan KC. Diffusion tensor imaging of visual pathway abnormalities in five glaucoma animal models. *Invest Ophthalmol Vis Sci* 2021;62(10):21.
- 39 Ji SL, Lin SY, Chen JS, Huang XP, Wei CC, Li ZY, Tang SB. Neuroprotection of transplanting human umbilical cord mesenchymal stem cells in a microbead induced ocular hypertension rat model. *Curr Eye Res* 2018;43(6):810-820.
- 40 Garcia-Herranz D, Rodrigo MJ, Subias M, Martinez-Rincon T, Mendez-Martinez S, Bravo-Osuna I, Bonet A, Ruberte J, Garcia-Feijoo J, Pablo L, Garcia-Martin E, Herrero-Vanrell R. Novel use of PLGA microspheres to create an animal model of glaucoma with progressive neuroretinal degeneration. *Pharmaceutics* 2021;13(2):237.
- 41 Liu Y, Wang JC, Jin X, Xin ZY, Wu X, Tong X, Tao Y, Wang DJ. A novel rat model of ocular hypertension by a single intracameral injection of cross-linked hyaluronic acid hydrogel (Healaflo<sup>®</sup>). *Basic Clin Pharmacol Toxicol* 2020;127(5):361-370.
- 42 Noailles A, Kutsyr O, Mayordomo-Febrer A, Lax P, López-Murcia M, Sanz-González SM, Pinazo-Durán MD, Cuenca N. Sodium hyaluronate-induced ocular hypertension in rats damages the direction-selective circuit and inner/outer retinal plexiform layers. *Invest Ophthalmol Vis Sci* 2022;63(5):2.
- 43 Erisgin Z, Ozer MA, Tosun M, Ozen S, Takir S. The effects of intravitreal H<sub>2</sub>S application on apoptosis in the retina and cornea in experimental glaucoma model. *Int J Exp Path* 2019;100(5-6):330-336.
- 44 Zhou RR, Li HB, You QS, Rong R, You ML, Xiong K, Huang JF, Xia XB, Ji D. Silencing of GAS5 alleviates glaucoma in rat models by reducing retinal ganglion cell apoptosis. *Hum Gene Ther* 2019;30(12):1505-1519.
- 45 Hvozda Arana AG, Lasagni Vitar RM, Reides CG, Calabró V, Marchini T, Lerner SF, Evelson PA, Ferreira SM. Mitochondrial function is impaired in the primary visual cortex in an experimental glaucoma model. *Arch Biochem Biophys* 2021;701:108815.
- 46 Kralj T, Kokot A, Zlatar M, Masnec S, Kasnik Kovac K, Milkovic Perisa M, Batelja Vuletic L, Giljanovic A, Strbe S, Sikiric S, Balog S, Sontacchi B, Sontacchi D, Buljan M, Lovric E, Boban Blagaic A, Skrtic A, Seiwert S, Sikiric P. Stable gastric pentadecapeptide BPC 157 therapy of rat glaucoma. *Biomedicines* 2021;10(1):89.
- 47 Liang X, Li N, Rong Y, Wang JM, Zhang H. Identification of proteomic changes for dexamethasone-induced ocular hypertension using a tandem mass tag (TMT) approach. *Exp Eye Res* 2022;216:108914.
- 48 Horng CT, Yang YL, Chen CC, Huang YS, Chen C, Chen FA. Intraocular pressure-lowering effect of *Cordyceps cicadae* mycelia extract in a glaucoma rat model. *Int J Med Sci* 2021;18(4):1007-1014.
- 49 Shepard AR, Millar JC, Pang IH, Jacobson N, Wang WH, Clark AF. Adenoviral gene transfer of active human transforming growth factor- $\beta_2$  elevates intraocular pressure and reduces outflow facility in rodent eyes. *Invest Ophthalmol Vis Sci* 2010;51(4):2067-2076.

- 50 Su Y, Cheng JL, Liu HT, Wang F, Zhao SG. Adenovirus conducted connective tissue growth factor on extracellular matrix in trabecular meshwork and its role on aqueous humor outflow facility. *Mol Biol Rep* 2013;40(11):6091-6096.
- 51 Tsukamoto T, Kajiwara K, Nada S, Okada M. Src mediates TGF- $\beta$ -induced intraocular pressure elevation in glaucoma. *J Cell Physiol* 2019;234(2):1730-1744.
- 52 Aragón-Navas A, Rodrigo MJ, Garcia-Herranz D, Martinez T, Subias M, Mendez S, Ruberte J, Pampalona J, Bravo-Osuna I, Garcia-Feijoo J, Pablo LE, Garcia-Martin E, Herrero-Vanrell R. Mimicking chronic glaucoma over 6 months with a single intracameral injection of dexamethasone/fibronectin-loaded PLGA microspheres. *Drug Deliv* 2022;29(1):2357-2374.
- 53 Rodrigo MJ, Bravo-Osuna I, Subias M, Montolio A, Cegoñino J, Martinez-Rincón T, Mendez-Martinez S, Aragón-Navas A, Garcia-Herranz D, Pablo LE, Herrero-Vanrell R, Del Palomar AP, Garcia-Martin E. Tunable degrees of neurodegeneration in rats based on microsphere-induced models of chronic glaucoma. *Sci Rep* 2022;12(1):20622.
- 54 Chang PY, Wang JK, Weng HY, Chang SW. Cataract surgery reduces intraocular pressure but not posture-induced intraocular pressure changes in patients with angle-closure glaucoma. *Sci Rep* 2019;9(1):14116.
- 55 Ferguson TJ, Dockter Z, Bleeker A, Karpuk KL, Schweitzer J, Ibach MJ, Berdahl JP. iStent inject trabecular microbypass stent implantation with cataract extraction in open-angle glaucoma: early clinical experience. *Eye Vis (Lond)* 2020;7:28.